

High porosity copper foam

S. XIE, J. R. G. EVANS

Department of Materials, Queen Mary, University of London, Mile end Road, London E1 4NS, UK

Recent interest in metallic or ceramic foams is reflected in two comprehensive reviews [1, 2]. Closed cell foams offer unique mechanical properties as a function of density. Open cell foams allow fluid transport in the pore structure and can be used for heat dissipation and recuperation, or as catalyst supports, or in filtration. Models for heat [3–5] and electrical [6, 7] transport in porous metals and reticulated structures are emerging.

Closed cell foams can be assembled by the sintering of hollow spheres, a method that has been applied to titanium and stainless steel [8]. Internal blowing agents such as dissolved gas [9, 10] or hydrogen produced by the decomposition of hydrides [11] can be used for foaming metals. Powder processing routes have been used widely for ceramic foams and are reviewed by Saggio-Woyansky *et al.* [12], Sepulveda [13], and Rice [2]. Many of these make use of the high porosity developed in polymeric foams. In the slurry infiltration method, polyurethane foam is used as a scaffold. After infiltration with powder slurry, it is dried and then fired to decompose the polyurethane and sinter the powder [14]. Polyurethane foam can also be used as a fugitive pattern for casting magnesium foams [15]. A traditional two-part polyurethane can be used as a vehicle for foaming a fine ceramic powder [16]. This method has been used for iron powder [17], and also for making foams of fine (3 μm diameter) alumina fibers to act as reinforcing preforms in metal matrix composites made by squeeze casting [18].

In the present work, copper foam was made by a powder metallurgy route by using polyurethane that is subsequently removed by heating in air. The copper foam structure is almost completely oxidised at the intermediate stage, but reduced on sintering to produce copper foams with porosities from 85 to 91%.

The powder was <53 μm gas atomised OHFC copper supplied vacuum, packed by Osprey Metals Ltd. (Neath, Wales). The foaming system consisted of a low silicone polyol resin, Flexocel SR300W with density 1030 kgm^{-3} and isocyanate based on diphenylmethane diisocyanate (MDI) grade 174 with density 1240 kgm^{-3} supplied by Bentley Chemicals Ltd. Kidderminster, UK.

The compositions were formulated to give nominally 0, 40, 45, 50 and 55 vol% based on a polyurethane theoretical density of 1150 kgm^{-3} [19] using a sample size of 75 g resin in each case. Powder sufficient to give the target volume fraction was mixed into each component of the foam separately at 2000 rpm with a high speed stirrer. The polyol and MDI suspensions of powder were then blended, stirred for 30 s and cast into shallow boxes that allowed unrestricted rise, to avoid

producing elongated cell structures. Samples were cut with a band saw to nominally 20 mm cubes and heated in air at 0.5 $^{\circ}\text{C/hr}$ to 650 $^{\circ}\text{C}$ on an alumina tile or shallow crucible, and held for 5 hrs before furnace cooling. A deep crucible was avoided because samples close to the bottom did not fully sinter. The powder assembly, now free from polymer but heavily oxidized, was then sintered in Ar/4% H_2 at 1000 $^{\circ}\text{C}$ for 4 hrs to produce bright copper foam samples (Fig. 1).

Table I gives the compositions and the actual mass fractions based on loss on ignition. The samples were weighed as-foamed and after reduction to copper during sintering. Mixing errors were due to dispensing small amounts of viscous fluid. The polyurethane can accommodate high volume fractions of coarse metal powder without loss of porosity on foaming. In contrast, with fine ceramic powders, the foam did not expand fully when the ceramic volume fraction rose above 25 vol% [16]. This is partly attributable to the wide particle size distribution of the copper, which means that extensional viscosity does not increase markedly until there are high solid contents. The theoretical densities of the copper-polyurethane solid phase (Table I: col. 4) allows the initial porosity to be found. The initial porosity of the unfilled foam was also recorded for comparison.

This is a low silicone polyurethane foam that produces a higher density product than the high porosity polyurethanes used for thermal insulation, and is more suited to motor vehicle applications. The unfilled foam porosity of 88.4% should be compared with values of $\sim 97\%$ for insulation foams.

The pyrolysis stage must be conducted in air otherwise residual organic material and carbon prevents sintering. Precautions are needed for the safe disposal of the exhaust gases from the furnace. Many powder metallurgy and ceramic binder removal ovens are now fitted with after-burners. The use of an inert atmosphere tends to produce fluid degradation products resulting in the partial collapse of the foam and hence was avoided. The copper was therefore converted almost completely to oxide, and then reduced at the sintering stage. This transition did not impair the foam, indeed it may be responsible for the slightly higher porosity in the sintered copper, compared with the metal-polymer foam. When the cell diameters are greater than the interparticle pore diameters, the foam should sinter as a macrostructure, and cell porosity should be retained on shrinkage. In this case, it is marginally higher due to distortions caused by the volume expansion on oxidation.

The microstructure of the 55 vol% copper composite (Fig. 2) shows the struts, windows and the

TABLE I Compositions and densities of foams

Initial nominal vol% Cu	Mass% Cu from LOI ^a (target mass)	Actual vol% Cu in polymer	Theoretical density of solid phase (kgm ⁻³)	As-formed density ^b (kgm ⁻³)	Porosity as formed (%)	Sintered density (kgm ⁻³)	Sintered foam porosity (%)
0	–	–	1150	134	88.3	–	–
40	83.0 (83.1)	38.6	4153	617	85.1	790	91.1
45	87.1 (86.0)	46.5	4770	763	84.0	817	90.9
50	90.5 (88.1)	55.0	8191	1079	86.8	1179	86.8
55	92.7 (90.3)	62.1	8362	1377	83.5	1311	85.3

^aLoss on ignition at 650 °C in air and sintering in Ar-4%H₂.

^bMin. no of samples: 5.



Figure 1 Sintered copper foam samples as approx. 20 mm cubes.

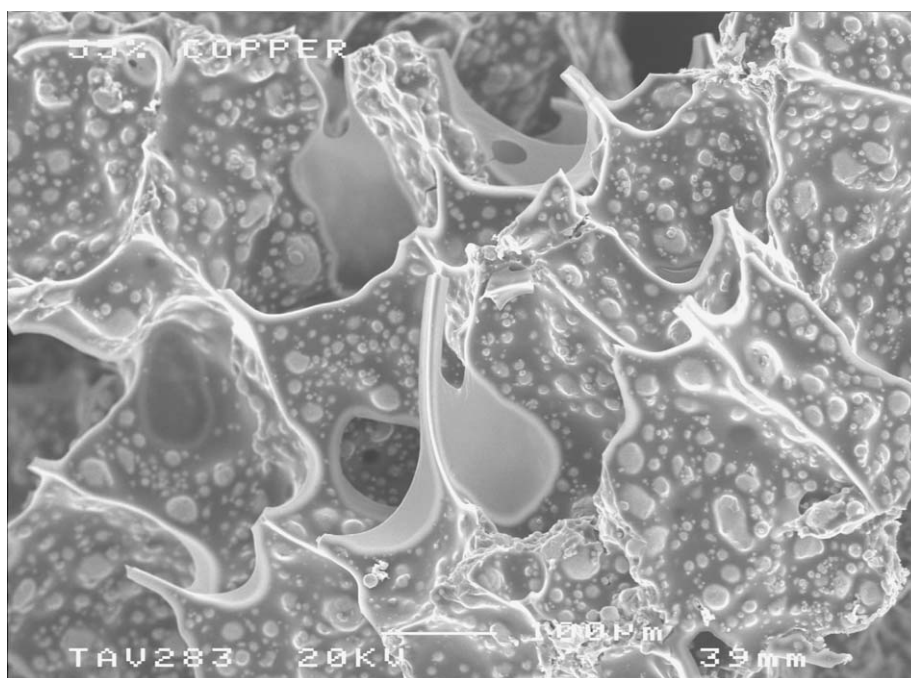


Figure 2 Fracture surface of a 55 vol% copper-polyurethane foam before sintering. The fracture surface was obtained after cooling the sample in liquid nitrogen.

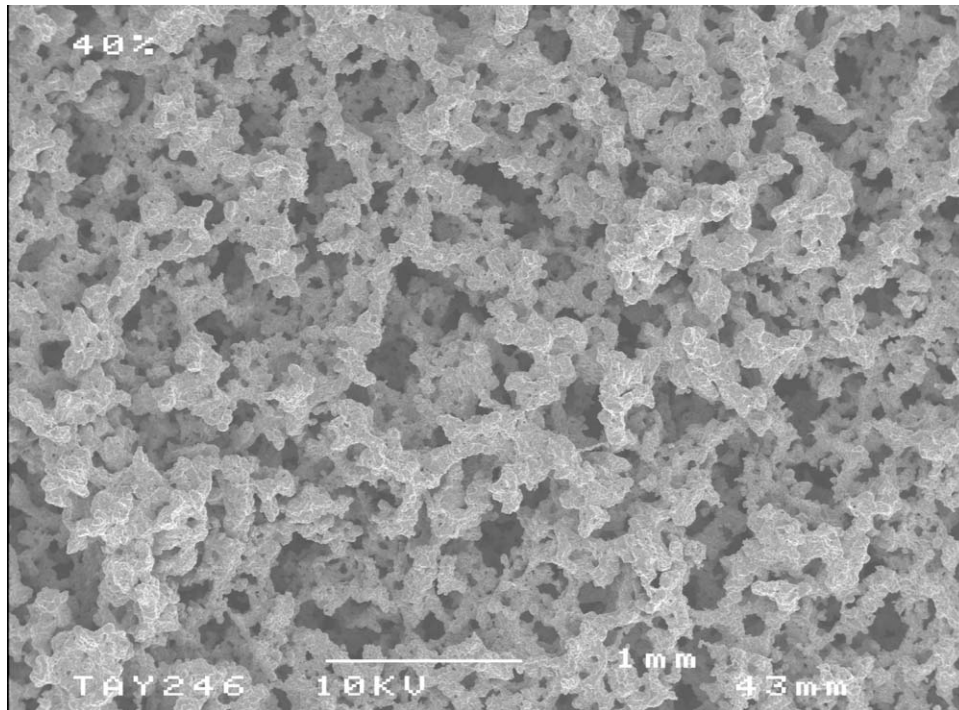


Figure 3 Sintered copper structure of a 91% porosity foam (from the 40 vol% suspension).

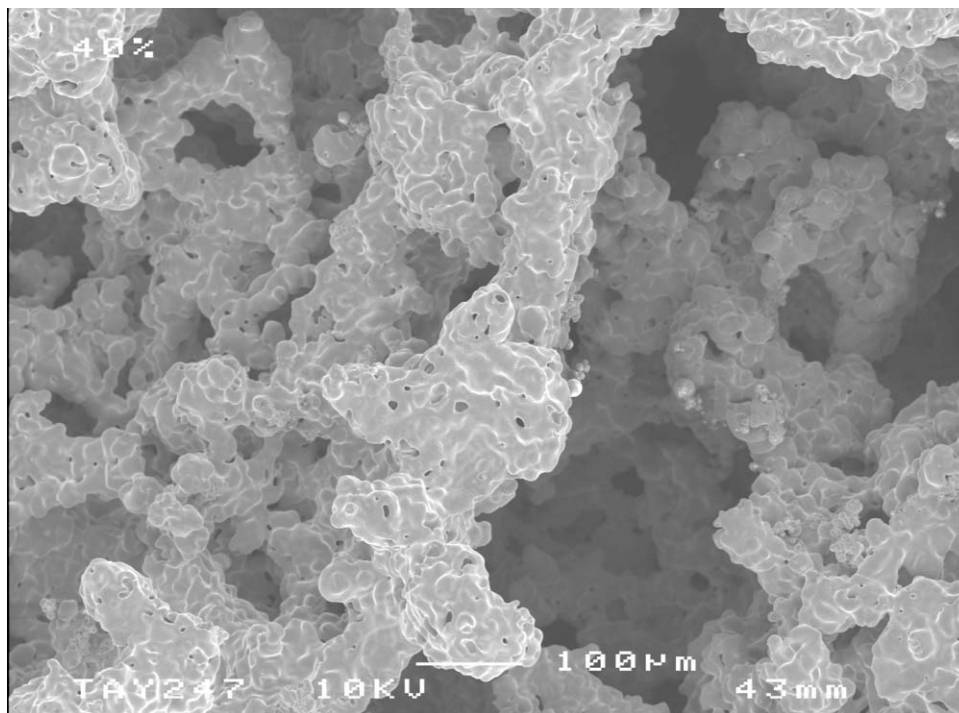


Figure 4 Higher magnification image of the arrangement of struts in a 91% porosity copper foam showing residual sintering porosity.

distribution of particles. Even at this high solids content, the particles do not restrict the expansion much; the porosity has been reduced by less than 5% (Table I). It is difficult to imagine how the structures such as that shown in Fig. 3 develop from apparently isolated particles but shrinkage, polymer loss, and copper oxidation, take place concurrently during pyrolysis of the polyurethane. The particles may be held in place by minor inorganic residues from the polymer as well as van der Waals forces. Reduction and sintering do not produce a fully dense system of

struts as shown in Fig. 4 despite the severe sintering conditions.

These foams are easily prepared and are sintered by conventional powder metallurgy methods. The macroporosity is retained, indeed slightly increased, on conversion to sintered copper. The result is porosity above 90% in an electrically conducting solid. Using the data and procedures in a review of apparent thermal conductivity in foams [20], at 90% porosity, the effect of increasing the solid phase conductivity from $0.25 \text{ Wm}^{-1} \text{ K}^{-1}$ (polyurethane) to $380 \text{ Wm}^{-1} \text{ K}^{-1}$

(copper) is to increase apparent conductivity from $0.025 \text{ Wm}^{-1}\text{K}^{-1}$ to $10 \text{ Wm}^{-1}\text{K}^{-1}$.

References

1. L. J. GIBSON and M. F. ASHBY, "Cellular Solids; Structure and Properties," 2nd ed. (CUP, Cambridge, UK, 1997).
2. R. W. RICE, "Porosity of Ceramics" (Marcel Dekker, N.Y., 1998).
3. J. T. DICKEY and G. P. PETERSON, *J. Energy Resources Tech.-Trans ASME* **119** (1997) 171.
4. T. J. LU, H. A. STONE and M. F. ASHBY, *Acta Mater* **46** (1998) 3619.
5. A. BATTACHARYA, V. V. CALMIDI and R. L. MAHAJAN, *Int. J. Heat Mass Trans.* **45** (2002) 1017.
6. K. P. DHARMASENA and H. N. G. WADLEY, *J. Mater. Res.* **17** (2002) 625.
7. J. KOVACIK and F. SIMANCIK, *Scripta Mater.* **39** (1998) 239.
8. K. M. HURYSZ, J. L. CLARK, A. R. NAGEL, C. U. HARDWICKE, K. J. LEE, J. K. COCHRANE and T. H. SANDERS, *Mater. Res. Symp.* **521** (1998) 191.
9. J. KOVACIK, *Acta Mater.* **46** (1998) 5413.
10. A. E. SIMONE and L. J. GIBSON, *J. Mater. Sci.* **32** (1997) 451.
11. J. BANHART and J. BAUMEISTER, *ibid.* **33** (1998) 1431.
12. J. SAGGIO-WOYANSKY, C. E. SCOTT and W. P. MINNEAR, *Amer. Ceram. Soc. Bull.* **71** (1992) 1674.
13. P. SEPULVEDA, *ibid.* **76** (1997) 61.
14. K. SCHWARTZWALDER and A. V. SOMERS, U. S. Patent No. 3,090,094, May 21, 1963.
15. Y. YAMADA, K. SHIMO, Y. SAKAGUCHI, M. MABUCHI, M. NAKAMURA, T. ASAHINA, T. MUKAI, H. KANAHASHI and K. HIGASHI, *J. Mater. Sci. Lett.* **18** (1999) 1477.
16. S. J. POWELL and J. R. G. EVANS, *Mater. Manuf. Proc.* **10** (1995) 757.
17. C. S. Y. JEE, N. ÖZGÜVEN, Z. X. GUO and J. R. G. EVANS, *Mat. Mater. Trans. B* **31B** (2000) 1345.
18. H. PENG, Z. FAN and J. R. G. EVANS, *J. Mater. Sci.* **36** (2001) 1007.
19. C. A. DOSTAL, "Engineered Materials Handbook" (Amer. Soc. Metals, Metals Park, Ohio, 1988) Vol. 2, p. 260.
20. P. G. COLLISHAW and J. R. G. EVANS, *J. Mater. Sci.* **29** (1994) 2261.

Received 3 February
and accepted 31 March 2004